Neuron
Article

SK2 Channel Modulation Contributes to Compartment-Specific Dendritic Plasticity in Cerebellar Purkinje Cells

Gen Ohtsuki,[1,2,4] Claire Piochon,[1] John P. Adelman,[3] and Christian Hansel[1,2,*]
[1]Department of Neurobiology, University of Chicago, Chicago, IL 60637, USA
[2]Department of Neuroscience, Erasmus University Medical Center, 3000 CA Rotterdam, The Netherlands
[3]Vollum Institute, Oregon Health & Science University, Portland, OR 97239, USA
[4]Present address: Department of Molecular Physiology, Kyushu University, Higashi-ku, Fukuoka, 812-8581 Japan
*Correspondence: chansel@bsd.uchicago.edu
http://dx.doi.org/10.1016/j.neuron.2012.05.025

SUMMARY

Small-conductance Ca^{2+}-activated K^+ channels (SK channels) modulate excitability and curtail excitatory postsynaptic potentials (EPSPs) in neuronal dendrites. Here, we demonstrate long-lasting plasticity of intrinsic excitability (IE) in dendrites that results from changes in the gain of this regulatory mechanism. Using dendritic patch-clamp recordings from rat cerebellar Purkinje cells, we find that somatic depolarization or parallel fiber (PF) burst stimulation induce long-term amplification of synaptic responses to climbing fiber (CF) or PF stimulation and enhance the amplitude of passively propagated sodium spikes. Dendritic plasticity is mimicked and occluded by the SK channel blocker apamin and is absent in Purkinje cells from SK2 null mice. Triple-patch recordings from two dendritic sites and the soma and confocal calcium imaging studies show that local stimulation limits dendritic plasticity to the activated compartment of the dendrite. This plasticity mechanism allows Purkinje cells to adjust the SK2-mediated control of dendritic excitability in an activity-dependent manner.

INTRODUCTION

Dendritic excitability is determined by the activity of voltage- and calcium-dependent ion channels that contribute to the input-output function of neurons (Häusser et al., 2000). Alterations in these active properties adjust dendritic integration and complement forms of synaptic plasticity, such as long-term potentiation (LTP) and long-term depression (LTD), in information storage (Daoudal and Debanne, 2003; Magee and Johnston, 2005; Zhang and Linden, 2003). For example, dendritic processing of intrinsic and synaptic signals is influenced by different calcium-activated K conductances (K_{Ca}) that may contribute to the after-hyperpolarization (AHP) following spike activity (Sah, 1996; Stocker et al., 1999) or accelerate the repolarization of excitatory postsynaptic potentials (EPSPs) (Lancaster et al., 2001). One class of (K_{Ca}), small conductance calcium-activated SK-type K channels act as a brake on dendritic responsiveness and calcium signaling. In hippocampus, blocking SK channels with apamin prolongs dendritic responses (Cai et al., 2004) and potentiates EPSP-spike coupling (Sourdet et al., 2003). In the amygdala and hippocampus, blocking synaptic SK channels enhances spine calcium transients leading to an increased probability for the induction of LTP (Faber et al., 2005; Lin et al., 2008; Ngo-Anh et al., 2005). In line with these observations, modulating SK channel activity influences hippocampus-dependent memory encoding (Hammond et al., 2006; Stackman et al., 2002). In cerebellar Purkinje cells, a form of intrinsic plasticity that is mediated by SK channel downregulation is associated with enhanced spine calcium transients, but in contrast to the hippocampus, this increased calcium signaling results in a lower probability for LTP induction (Belmeguenai et al., 2010; Hosy et al., 2011), possibly reflecting different calcium signaling requirements for hippocampal and cerebellar LTP (Coesmans et al., 2004). We used dendritic patch-clamp recordings from rat Purkinje cells in freshly prepared brain slices and found that SK channel downregulation affects the processing of activity patterns in Purkinje cell dendrites, enhancing their intrinsic excitability (IE). The excitability of Purkinje cell dendrites can be altered in response to either synaptic or nonsynaptic tetanization patterns. This increased dendritic IE leads to a long-term amplification of three types of dendritic responses: Na^+ spikes that passively spread into the dendrite (Llinás and Sugimori, 1980; Stuart and Häusser, 1994), dendritic responses to CF activation, and PF-EPSP trains. This type of long-lasting dendritic plasticity can be observed for the duration of the recordings (which lasted up to 30 min after tetanization). The amplification of CF responses is mimicked and occluded by apamin, an SK channel blocker. Moreover, dendritic plasticity is absent in SK2 null mice, suggesting that the increased IE is due to SK2 channel modulation. Using confocal calcium imaging and triple-patch recordings from the soma and two dendritic locations we show that the increase in CF responses may be restricted to locally activated compartments of the dendrite. Activity-dependent plasticity of dendritic IE thus requires SK2 channel regulation and allows Purkinje cells to locally adjust dendritic processing properties.

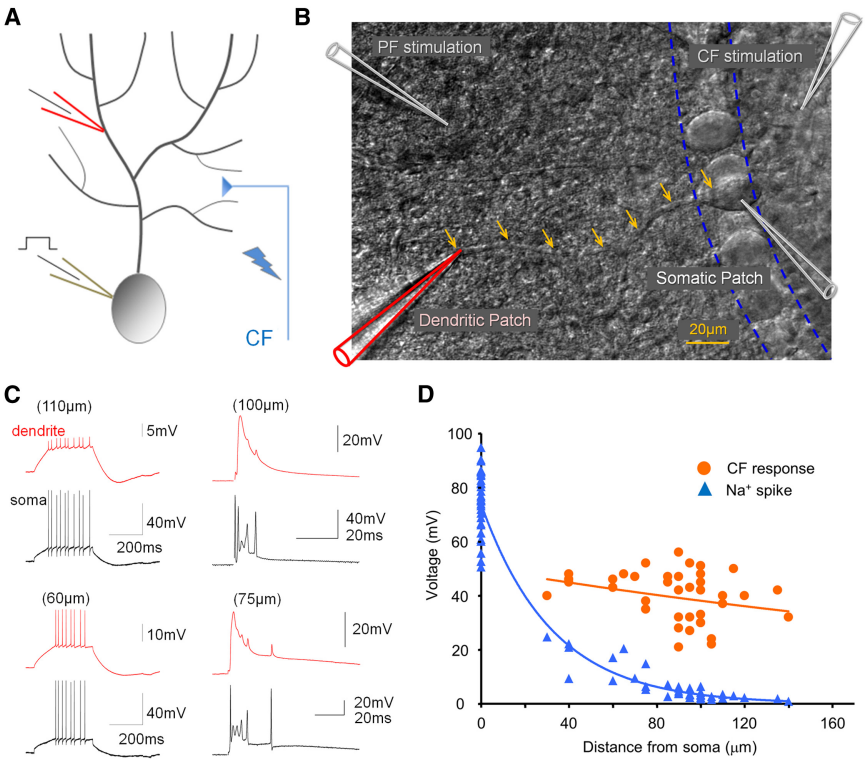

Figure 1. Depolarization-Evoked Na^+ Spikes and CF Responses in Somatodendritic Double-Patch Recordings

(A) Recording configuration. Patch-clamp recordings were obtained from the soma and the dendrite of Purkinje cells. Depolarizing current pulses were applied through the somatic patch electrode. The CF input was activated using extracellular stimulation with a glass pipette filled with ACSF.

(B) DIC image illustrating the double-patch configuration. Arrows outline the course of the primary dendrite. Glass pipettes for PF and CF stimulation, respectively, are shown in the upper left and right corners.

(C) Examples of Na^+ spikes evoked by somatic depolarization (left) and CF responses (right) recorded at dendritic locations (red traces) and the soma (black traces).

(D) Distance dependence of Na^+ spike (blue) and CF response (orange) amplitudes. The fitted lines were obtained using the least-square method.

RESULTS

Activity-Dependent Changes in Excitability Boost Dendritic Responsiveness

To measure spike activity and synaptic responses in Purkinje cell dendrites, we performed dual somatic and dendritic patch-clamp recordings (Davie et al., 2006) from Purkinje cells in cerebellar slices obtained from P25–P37 rats. Na^+ spikes evoked by somatic depolarization, or synaptic responses to CF stimulation were monitored at near-physiological temperature (31°C–34°C). As previously reported, the amplitude of Na^+ action potentials decreased with distance from the soma (Pearson's correlation coefficient after log transformation of the Na^+ spike amplitude: $r = -0.8923$; $p < 0.05$; $n = 42$; Figures 1A–1D), suggesting that in Purkinje cells Na^+ spikes passively spread into the dendrite (Llinás and Sugimori, 1980; Stuart and Häusser, 1994). CF stimulation evoked complex spike discharges in the soma, but not the dendrite. Rather, the dendritic recordings showed large CF-evoked EPSPs that did not vary in amplitude with distance from the soma ($r = -0.2645$; $p > 0.05$; $n = 39$; Figures 1A–1D). The dendritic CF responses often contained small spike components that have been attributed to passively spreading Na^+ spikelets and to local calcium spike activity (Figure 1C; Davie et al., 2008; Ohtsuki et al., 2009).

To determine how alterations of IE may regulate dendritic responsiveness and Purkinje cell output, CF and PF responses as well as Na^+ spikes were measured, using double-patch experiments, before and after inducing plasticity of IE. The dendritic recordings were obtained 50–140 μm from the soma (from the point of origin of the dendrite). Dendritic responses to CF stimulation reached an averaged amplitude of 32.67 mV ± 2.93 SEM ($n = 40$; averaged baseline values from all rat recordings; see Table S1 available online). To induce plasticity of IE, depolarizing currents (300–400 pA/100 ms) were injected into the soma at 5 Hz for 3–4 s, a tetanization protocol that triggers IE plasticity in Purkinje cells (Belmeguenai et al., 2010). Following 5 Hz current injection, the amplitude of dendritic CF responses was enhanced (123.2% ± 8.4% of baseline; last 5min; $n = 7$; $p = 0.032$; Figures 2A and 2B). The degree of enhancement did not depend on the distance of the dendritic recording site from the soma (Figure S1). The enhancement of dendritic CF response amplitudes was associated with an increase in the number of spikelets within the somatically recorded complex spike (144.8% ± 3.7%; $n = 7$; $p = 0.028$; Figure 2B). Under control conditions, these parameters remained stable (amplitude: 97.0% ± 5.9%; $p = 0.636$; spikelet number: 102.6% ± 5.3%; $n = 6$; $p = 0.652$; Figures 2B and S2). Repeated current injection did not result in significant input resistance changes (dendrite: 90.2% ± 8.2%; $p = 0.276$; soma: 96.3% ± 6.9%; $p = 0.613$; $n = 7$; Figure S3). Patch-clamp recordings from the rat cerebellum in vivo show that sensory stimulation results in brief high-frequency bursts in granule cells, identifying a physiologically relevant activity pattern of PF synaptic signals (Chadderton et al., 2004). PF burst stimulation (50Hz bursts; 5 pulses; repeated at 5Hz for 3 s) caused an increase in the CF response (112.2% ± 2.7%; $p = 0.010$) that was associated with an increase in the spikelet number (128.7% ± 9.6%; $n = 5$; $p = 0.040$; Figures 2C and 2D). Moreover, the PF burst protocol enhanced the number of depolarization-evoked spikes (Figure S4). Taken together, these data show that dendritic plasticity can be triggered by synaptic or nonsynaptic activity patterns. Repeated depolarizing current injections into the soma also increased the amplitude of dendritic Na^+ spikes that were elicited by somatic test current pulses (139.5% ± 15.2%; $n = 10$;

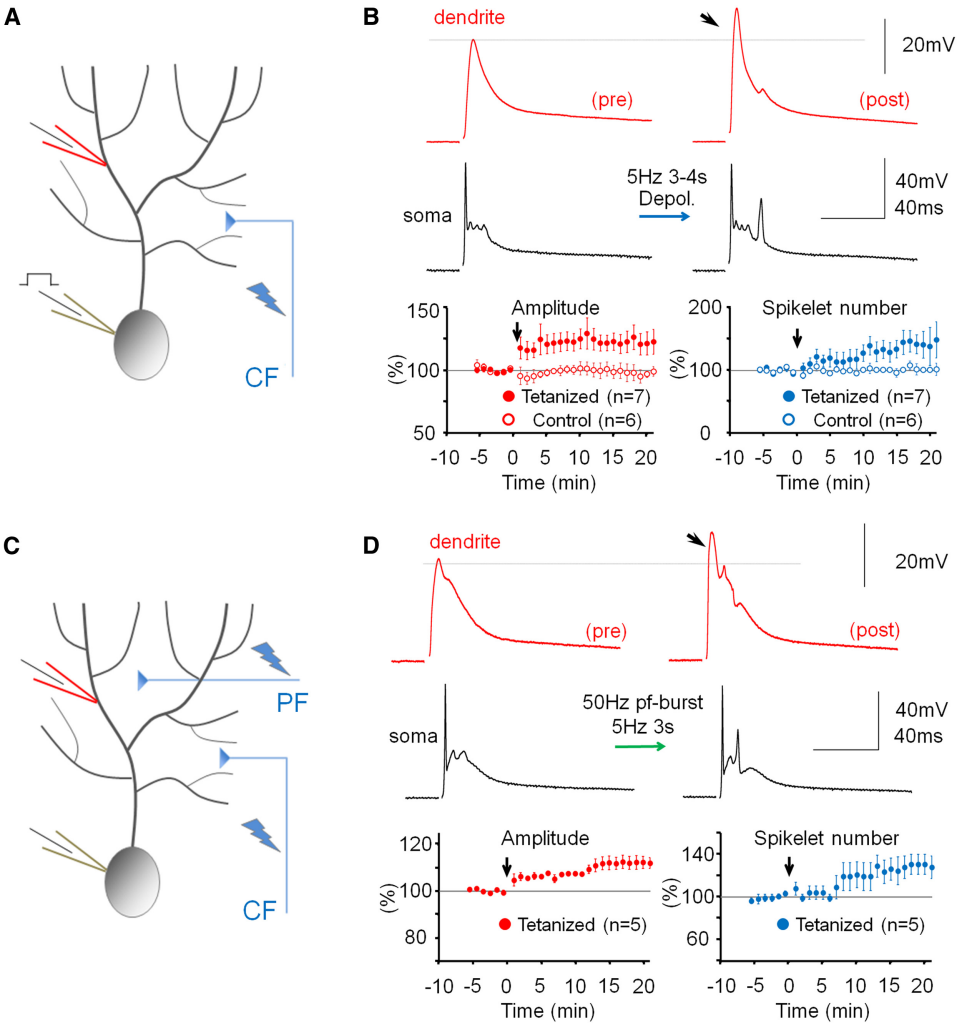

Figure 2. Dendritic Patch-Clamp Recordings Reveal Activity-Dependent Changes in Dendritic Responsiveness

(A) Recording configuration for the experiments shown in (B). Responses to CF activation were recorded before and after repeated injection of depolarizing currents into the soma.

(B) The somatic depolarization protocol enhances CF responses (arrow). Lower left: time graph showing changes in the amplitude of dendritically recorded CF responses after tetanization (closed dots; n = 7) and under control conditions (open dots; n = 6). Lower right: time graph showing associated changes in the number of spikelets in the complex spike after tetanization (closed dots; n = 7) and under control conditions (open dots; n = 6).

(C) Recording configuration for the experiments shown in (D). Responses to CF activation were recorded before and after 50 Hz PF tetanization.

(D) 50 Hz PF burst stimulation causes an increase in dendritic CF response amplitudes (lower left) and the spikelet number (lower right; n = 5). Arrows indicate tetanization. Error bars indicate SEM.

See also Figures S1–S4 and Table S1.

p = 0.029; Figure 3). This enhancement was accompanied by an increase in the number of evoked spikes (spike count) in somatic and dendritic recordings (179.4% ± 29.7%; n = 10; p = 0.028; Figure 3). Under control conditions, both the dendritic spike amplitude (96.7% ± 8.3%; p = 0.711) and the spike count remained constant (105.5% ± 10.1%; n = 5; p = 0.613; Figures 3 and S2). The finding that somatic depolarization, a nonsynaptic activation protocol, causes an increase in the amplitude of dendritic Na^+ spikes, a nonsynaptic response, indicates that the underlying process involves modifications of intrinsic membrane properties, and that this modification occurs in Purkinje cells.

Dendritic Plasticity Requires SK2 Channel Downregulation

SK channel activity influences Purkinje cell firing frequency and regularity (Edgerton and Reinhart, 2003; Womack and Khodakhah, 2003). It has previously been shown that Purkinje cell intrinsic plasticity, measured as an increase in the number of spikes evoked by depolarizing current pulses, involves SK channel downregulation (Belmeguenai et al., 2010). To examine whether the changes in dendritic Na^+ spike and CF response amplitudes described here are also mediated by downregulation of SK channel activity, we used the selective SK channel blocker, apamin. Bath-application of apamin (10nM) enhanced the

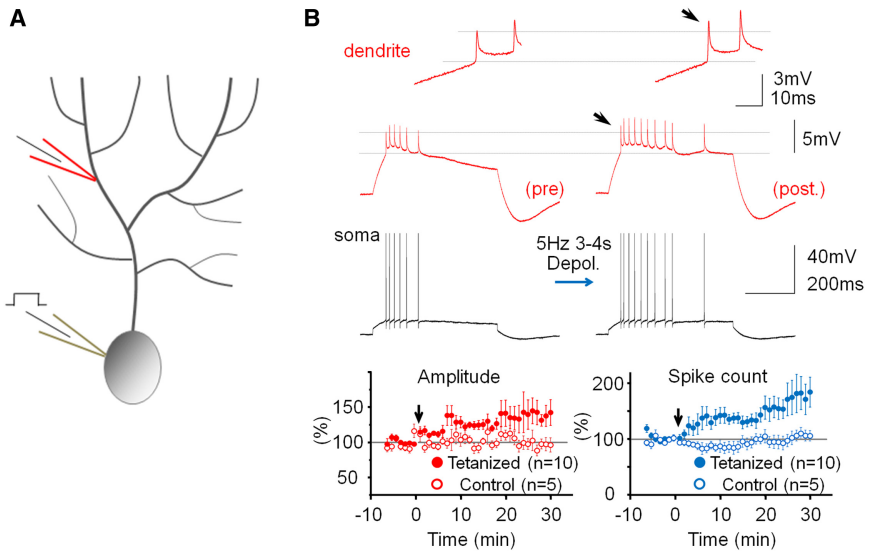

Figure 3. Repeated Somatic Injection of Depolarizing Currents Enhances the Frequency and Dendritic Amplitude of Na^+ Spikes

(A) Recording configuration. Na^+ spikes evoked by single depolarizing current pulses injected into the soma were recorded in the test periods before and after repeated somatic current injection at 5 Hz.

(B) The depolarization protocol enhances the number of action potentials and the amplitude of dendritic Na^+ spikes (red traces; enlarged in the insets). Lower left: time graph showing Na^+ spike amplitude changes recorded in the dendrite after tetanization (closed dots; n = 10) and under control conditions (open dots; n = 5). Lower right: time graph showing associated changes in the spike count after tetanization (closed dots; n = 10) and under control conditions (open dots; n = 5). Arrows indicate tetanization. Error bars indicate SEM. See also Figure S2.

amplitude of dendritic CF responses (119.0% ± 6.2%; p = 0.028; Figure 4A) and the number of spikelets in the somatic complex spike (137.5 ± 14.1; n = 6; p = 0.045; Figure 4A). In the presence of apamin, repeated depolarizing current injections (5 Hz; 3–4 s) neither caused a significant increase in CF response amplitudes (98.0% ± 2.1%; p = 0.373), nor in the spikelet number (120.3% ± 16.4%; n = 6; p = 0.283; Figure 4B). These observations show that plasticity of IE was, at least partially, occluded by apamin blockade of SK channels. Apamin also increased the amplitude of dendritically recorded Na^+ spikes (151.9% ± 21.6%; p = 0.043), as well as the spike count (222.8% ± 16.9%; n = 9; p = 0.00009; Figure 4C). SK2 (Kcnn2) is the only member of the SK family expressed in Purkinje cells (Cingolani et al., 2002). To directly test the role of SK2 channels in dendritic plasticity, we performed dual patch-clamp recordings from SK2 null ($SK2^{-/-}$) mice (Bond et al., 2004) or wild-type littermates (P17–P35). In these mouse experiments, dendritic recordings were obtained 40–110 μm from the soma. Dendritic responses to CF stimulations had amplitudes of 20.59 ± 6.27mV (n = 10). Application of the depolarization protocol caused a significant increase in CF response amplitudes for wild-type (137.5% ± 14.4%; n = 6; last 5min; p = 0.048; Figure 4D) but did not elicit an increase of CF responses in $SK2^{-/-}$ mice (84.7% ± 14.9%; n = 4; p = 0.379; Figure 4D). The difference between these two groups was significant (p = 0.01; Mann-Whitney U test). These results specifically implicate SK2 channels in this form of intrinsic plasticity. CF stimulation from $SK2^{-/-}$ mice frequently triggered prolonged spike firing rather than an isolated complex spike, preventing an accurate measure of the spikelet number. In summary, experiments in the presence of apamin as well as the recordings from $SK2^{-/-}$ mice and wild-type littermates show that the increase in dendritic IE depends on a decrease of SK2 channel activity. The apamin wash-in experiments show that SK channel blockade, in the absence of tetanization, causes a similar excitability increase, suggesting that a reduction in SK2 channel activity underlies, at least in part, the expression mechanism for this type of intrinsic plasticity.

Dendritic Plasticity Affects PF-EPSP Trains, but Not Individual EPSPs

To examine the effect of dendritic plasticity on PF synaptic responses, we applied 10 Hz stimulation (5 pulses) to the PF input, resulting in a train of EPSPs with amplitudes that increased over the first responses. Stimulus strength was adjusted so that the first EPSP in the train was of low amplitude and remained subthreshold (dendritic EPSP 1 = 1.4 ± 0.37mV; n = 9; Figures 5A and 5B). In the somatic recordings, action potentials appeared toward the end of the EPSP trains, which were also seen as small spikelets on top of the dendritically recorded EPSPs (Figure 5B). Depolarizing current injections (5 Hz, 3–4 s) did not change the amplitude of EPSP 1 (dendrite: 99.7% ± 19.3%; p = 0.988; soma: 104.5% ± 6.4%; p = 0.868; n = 9; Figure 5B), but significantly amplified the facilitation of EPSPs 2–5 in both dendritic and somatic recordings (% change EPSP 5 relative to EPSP 1; dendrite; before: 207.9% ± 17.6%; after: 356.2% ± 44.9%; n = 9; p = 0.011; soma; before: 182.9% ± 16.6%; after 336.8% ± 65.2%; n = 9; p = 0.036; Figure 5D). When 5 PF pulses were applied at 50 Hz (dendritic EPSP 1 = 0.91 ± 0.12mV; n = 8; Figure 5C) we observed a similar EPSP facilitation, which, however, resulted in more pronounced spike activity in the dendritic recordings (Figure 5C), rendering analysis of EPSP amplitudes impractical. After repeated current injections, the number of spike components per EPSP was significantly increased for EPSPs 4 + 5 (n = 8; EPSP 4: p = 0.040; EPSP 5: p = 0.036; Figure 5E). In the presence of apamin (10 nM), the EPSP increase during a 10 Hz EPSP train was enhanced as compared to control (% change EPSP 5 relative to EPSP 1; dendrite; control: 229.6% ± 25.2%; n = 10; apamin: 322.8% ± 12.9%; n = 7; p = 0.006; soma; control: 193.2% ± 12.7%; n = 10; apamin: 304.8 ± 15.8; n = 7; p = 0.0001; Figures 6A and 6C). In the presence of apamin, the number of spikes evoked by EPSPs 4+5 in a 50Hz train was also increased compared to control (control: n = 10; apamin: n = 7; EPSP 4: p = 0.015; EPSP 5: p = 0.042; Figures 6B and 6D). These observations show that dendritic plasticity does not affect single

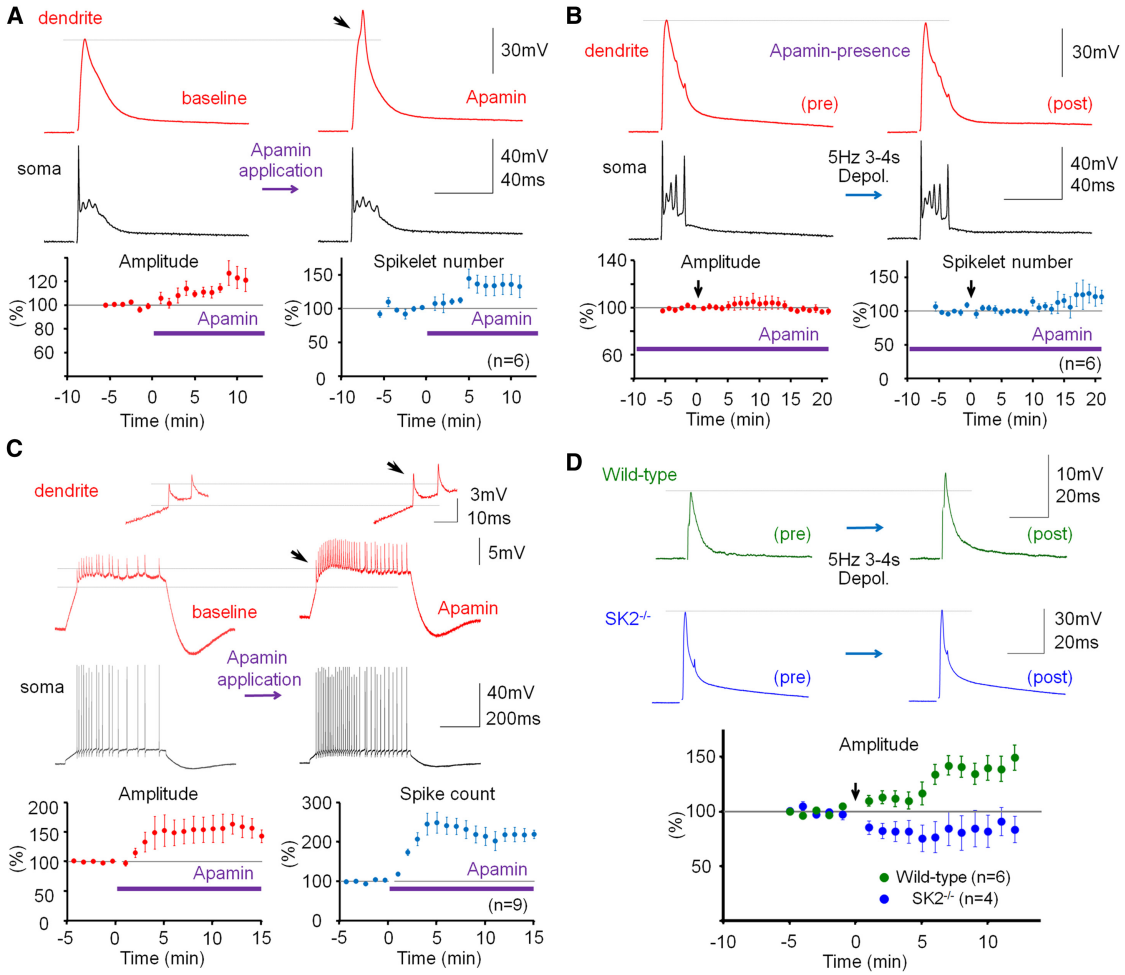

Figure 4. Dendritic Plasticity Is Mediated by SK2 Channel Downregulation

(A) Bath application of the SK channel blocker apamin (10 nM) enhances CF responses. Lower left: time graph showing changes in dendritic CF response amplitudes (red dots). Lower right: time graph showing changes in the spikelet number (blue dots; n = 6).

(B) In the presence of apamin in the bath, dendritic plasticity (depolarization protocol) is occluded. Lower left: time graph showing dendritic CF responses (red dots) when apamin was present in the bath. Lower right: time graph showing spikelet number changes (blue dots; n = 6).

(C) Apamin application enhances the spike count and the dendritic Na^+ spike amplitude (red traces; enlarged in the insets). Lower left: time graph showing changes in the Na^+ spike amplitude (n = 9). Lower right: time graph showing spike count changes (n = 9). Bars indicate the presence of apamin in the bath.

(D) Dendritic plasticity is absent in *SK2*$^{-/-}$ mice, but can be elicited in WT littermates. Top: typical traces obtained before (left) and after tetanization (right) from WT (top row) and *SK2*$^{-/-}$ Purkinje cells (bottom row). Bottom: time graph showing changes in dendritic CF response amplitudes in *SK2*$^{-/-}$ mice (blue dots; n = 4; n = 5 up to t = 4 min) and WT mice (green dots; n = 6).

The recording configuration for (A), (B), and (D) corresponds to the configuration shown in Figure 2A. The recording configuration for (C) corresponds to the configuration shown in Figure 3A. Arrows indicate tetanization. Error bars indicate SEM. See also Figure S3.

PF-EPSPs, but increases EPSP trains, thereby enhancing the probability that strong PF inputs reach spike threshold. A similar amplification is seen in the presence of apamin, suggesting that SK channel downregulation enhances PF burst signaling.

Dendritic Plasticity Can Be Restricted to Selectively Activated Compartments

The data show that dendritic responses as diverse as CF-evoked potentials, PF-EPSP trains and Na^+ spikes can be amplified, via downregulation of SK2 channel activity, by spatially unspecific activation patterns such as somatic depolarization or strong PF activation, suggesting that this type of dendritic plasticity can occur throughout large neuronal domains. Consistent with this, immunostaining shows SK2 expression throughout the Purkinje cell dendrite (Belmeguenai et al., 2010). To determine whether dendritic plasticity may be restricted to selectively activated areas of the dendritic tree, we performed triple-patch experiments in which recordings were simultaneously obtained from two distinct dendritic locations and the soma. The two dendritic patch electrodes were either placed on two different branches (Figures 7A and 7B), or on the same branch, but at different distances from the soma (Figure 7C). Figure 7D shows depolarization-evoked Na^+ spikes (left) and synaptically evoked CF responses (right) that were monitored on the same branch. As

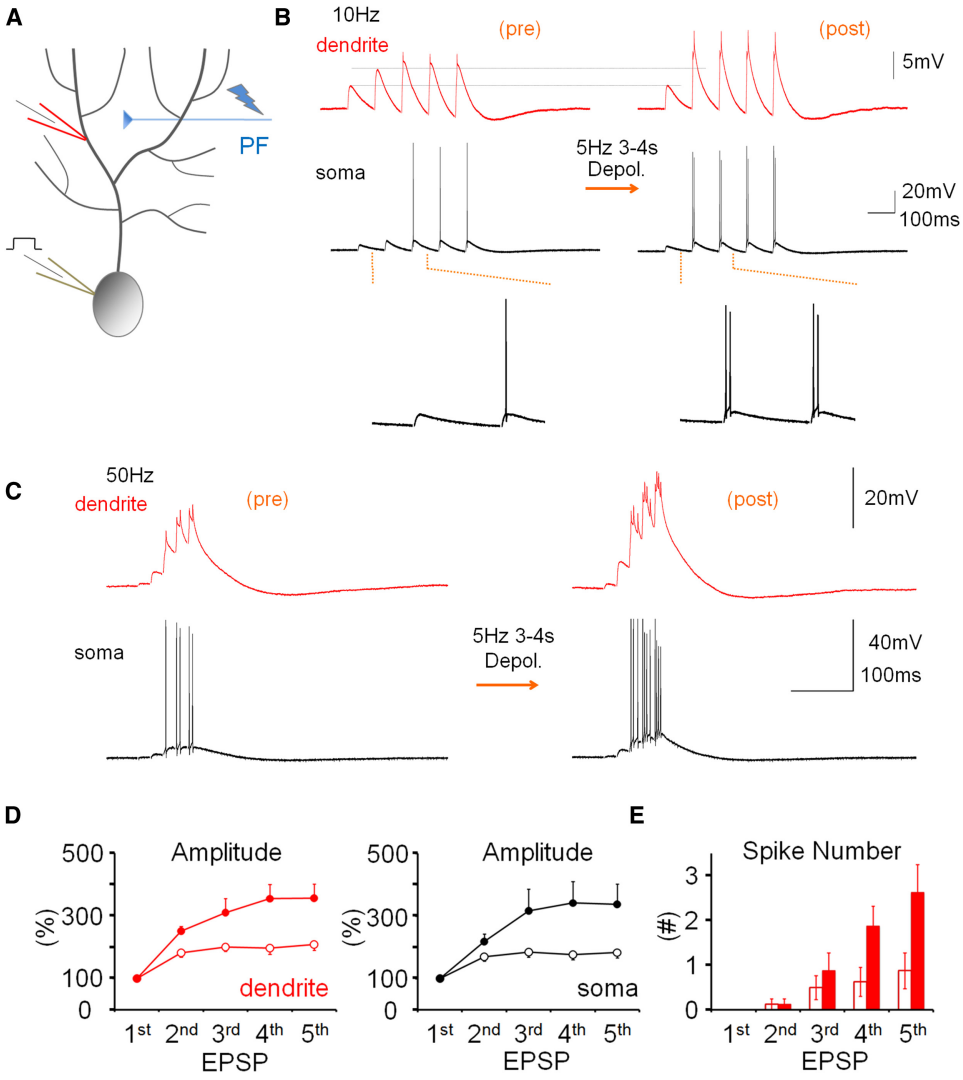

Figure 5. Dendritic Plasticity Enhances Parallel Fiber Burst Signaling

(A) Recording configuration. PF responses were measured before and after application of the somatic depolarization protocol.

(B) Repeated somatic depolarization does not alter the first EPSP in a 10 Hz EPSP train but enhances amplification of subsequent EPSPs. Left traces: dendritic (red) and somatic (black) baseline responses. Right traces: 20 min after tetanization.

(C) Tetanization enhances the facilitation within 50 Hz EPSP trains.

(D) EPSP facilitation within 10Hz trains before (open dots) and after tetanization (closed dots) in the dendrite (left) and soma (right; n = 9). In the presence of spikes, the EPSP amplitude was measured as the amplitude of the slow response component. EPSP amplitudes were normalized to the amplitude of EPSP 1 in the same train.

(E) The probability of spike firing was enhanced for the late EPSPs within a 50 Hz EPSP train (n = 8). The PF-EPSP train measures were obtained during the experiments shown in Figures 2B and 3. Three to nine sweeps were collected at minutes −10 to −7 (baseline), three sweeps were collected at minute −1 (before tetanization), and nine sweeps or more were collected at minutes +20 to 30 (after tetanization). Error bars indicate SEM.

predicted from double-patch recordings performed at various distances from the soma (Figures 1A–1D), the Na^+ spike amplitude was smaller at more distal dendritic locations (here 125 μm as compared to 70 μm), whereas the CF response amplitude was distance independent. To simultaneously monitor dendritic gain changes at two separate dendritic locations, we performed triple-patch recordings of CF responses (n = 5; in three recordings the two dendritic patch electrodes were placed on different branches of the dendrite as shown in Figure 7B). We took advantage of CF responses because of their large amplitudes (advantage over dendritic Na^+ spikes) and because they can be equally well recorded on different branches of the dendrite (advantage over the spatially restricted PF responses). To selectively activate one recording site, we used modified versions of the two protocols described above: (1) depolarizing current pulses injected through one of the dendritic patch electrodes, rather than into the soma, (2) 50 Hz PF stimulation protocol, with the stimulus electrode placed lateral to the

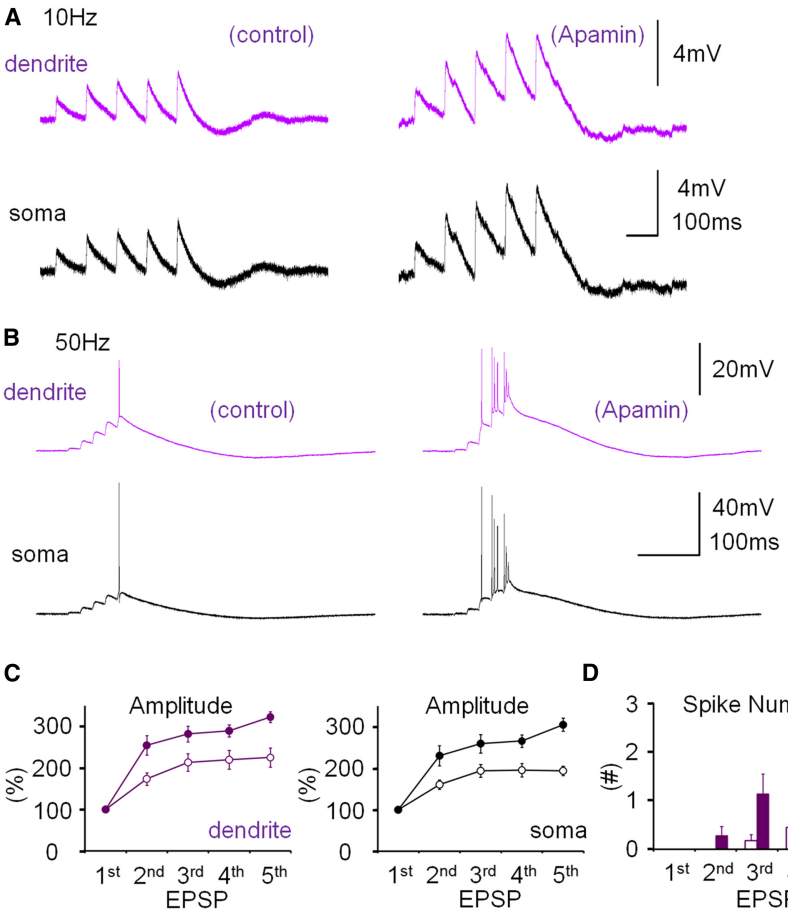

Figure 6. Apamin Bath Application Enhances Parallel Fiber Burst Signaling

(A) When apamin was bath applied, the EPSP amplification within a 10 Hz EPSP train was enhanced (n = 10) as compared to control (n = 7). The recording configuration corresponds to the configuration shown in Figure 5A, but in the experiments shown here no tetanization protocol was applied. The traces shown on the right were recorded 20min after wash-in of apamin.

(B) In the presence of apamin in the bath, EPSP facilitation was observed in 50 Hz EPSP trains.

(C) EPSP facilitation under control conditions (open dots; n = 7) and in the presence of apamin (10 nM; closed dots; n = 10) in the dendrite (left; purple dots) and the soma (right; black dots).

(D) The facilitation within 50 Hz trains resulted in an enhanced spike number in the late EPSPs (control: n = 7; apamin: n = 10). Error bars indicate SEM.

dendritic target area (for an example, see Figure 7B), and the stimulus intensity adjusted to evoke smaller PF-EPSPs (n = 5; depolarization: n = 2; 50 Hz PF tetanization: n = 3). In comparison to the dendritic responses obtained with 50 Hz PF stimulation in the previous recordings (12.5 ± 1.0 mV; n = 5; Figure 2D), in which the stimulus electrode was randomly placed in the molecular layer, application of the modified PF tetanization protocol resulted in smaller peak response amplitudes (5.3 ± 0.7 mV; n = 3; p = 0.036; Mann-Whitney U test). For simplicity, we use the terms "strong" and "weak" in this study, referring to the dendritic response strength, to address these two induction protocols. Figure 7E shows an example of weak PF activation resulting in an EPSP train at the conditioned site (red trace), but not at the unconditioned site (blue trace). For comparison, the gray trace on top shows a 50 Hz EPSP train evoked by strong PF activation. Figure 7F shows typical responses to the depolarization protocol. For both protocols, the peak depolarization at the conditioned site was significantly larger than at the unconditioned site (conditioned: 5.5 ± 0.5 mV; unconditioned: 1.6 ± 1.4 mV; n = 5; p = 0.042; Figure 7G). In both conditions, we observed a selective increase in the CF response amplitude at the activated dendritic recording site (134.7% ± 11.6%; n = 5; last 5 min; p = 0.013; paired Student's t test), while at the unconditioned site the responses were not significantly affected (82.7% ± 11.5%; n = 5; p = 0.207; Figures 7H and 7I). These data show that dendritic plasticity can selectively occur at dendritic locations that receive sufficient activation.

To obtain a second measure of compartment-specific dendritic plasticity, we performed confocal imaging experiments. The experimental layout was similar to the triple-patch recordings in that CF-evoked complex spikes were measured in the soma using patch-clamp recordings, and local CF responses were monitored in the dendrites. However, in this case, dendritic CF responses were measured using calcium transients. Purkinje cells were loaded with the green, calcium-sensitive fluorescent dye Oregon Green BAPTA-2 (200 μM; excitation wavelength: 488nm) and the red, calcium-insensitive fluorescent dye Alexa 633 (30 μM; excitation wavelength: 633 nm; Figure 8A). Calcium transients were calculated as $\Delta G/R = (G(t) - G_0)/R$ (Yasuda et al., 2004), where G is the green fluorescent signal of Oregon Green BAPTA-2 (G_0 = baseline signal) and R is the red fluorescent signal of Alexa 633. CF stimulation (2 pulses; 50 ms interval) evoked complex spikes (Figures 8B and 8C) which were associated with widespread calcium transients that could be recorded throughout large parts of the dendritic tree (Figure 8D). To trigger excitability changes, we applied the local 50 Hz PF tetanization (weak protocol) as used in the triple-patch recordings. A first region of interest (ROI) for calcium measurements was chosen within a distance of $\leq$ 10 μm from the stimulus electrode. This ROI-1 represents the conditioned site. Additional ROIs were selected at greater distances, with values determined relative to the center of ROI-1 (measured along the axis of the connecting dendritic branch). As shown in Figures 8E and 8F, local 50 Hz PF tetanization caused a pronounced calcium transient in ROI-1, but not at two ROIs that were located at distances of 29.8 and 50.2 μm, respectively, from ROI-1 (Figure 8A). Following tetanization, CF-evoked calcium transients recorded at ROI-1 were enhanced, but calcium signals monitored at

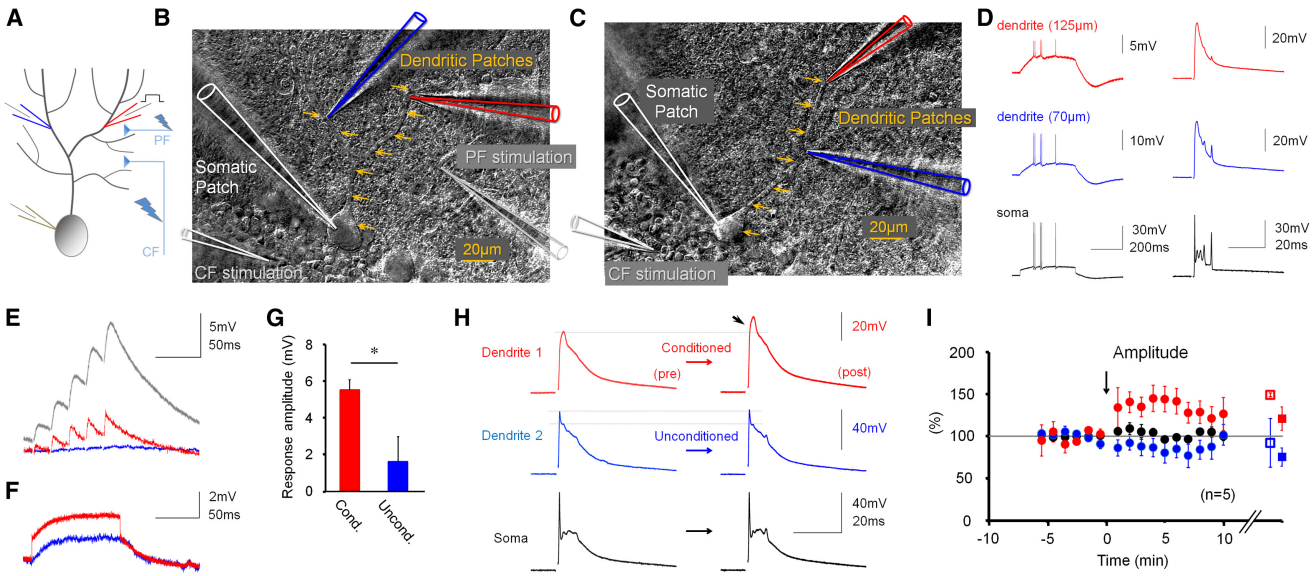

Figure 7. Triple-Patch Recordings Reveal Location-Specific Dendritic Plasticity

(A) Recording configuration. CF responses were recorded in two dendritic locations and the soma before and after either weak PF activation or repeated current injection at one of the dendritic recording sites.

(B) DIC image showing how simultaneous recordings are obtained from two different branches (blue and red patch pipettes), and the soma (white).

(C) DIC image showing the second configuration, in which recordings were obtained from two sites on the same branch. In (B) and (C), arrows indicate the course of the primary dendrite.

(D) Responses to somatic depolarization (left) and CF stimulation (right). These recordings were obtained at two sites on the same branch (70 and 125 µm).

(E) Example of responses to weak 50 Hz PF activation at the conditioned (red trace) and the unconditioned site (blue trace). For comparison, the gray trace on top shows a typical response resulting from strong 50 Hz PF activation as used for global excitability changes.

(F) Example responses to current injection (+80 pA) at one recording site (red trace), but not the other (blue trace).

(G) Bar graphs showing response amplitudes monitored at the conditioned and the unconditioned dendritic recording site (n = 5).

(H) The increase in CF response amplitudes was restricted to the locally conditioned (here: PF tetanization protocol) recording site (red traces), while CF responses recorded at the unconditioned site (blue traces) remained unchanged.

(I) Time graph showing changes in CF response amplitudes at the conditioned dendritic site (red dots), the unconditioned site (blue dots) and the soma (black dots; n = 5). On the right, the amplitude changes are separately shown for the two stimulus protocols (average: last 5 min; 50 Hz PF bursts: closed squares; n = 3; depolarization: open squares; n = 2). The arrow indicates tetanization. Error bars indicate SEM.

ROIs 2 and 3 were not (Figure 8D). On average, PF tetanization resulted in an increase in the peak amplitude and the area under the curve of calcium transients recorded at ROI-1 (peak: 130.5% ± 9.0%; p = 0.010; area: 165.7% ± 13.1%; p = 0.001; n = 9; t = 10–15 min; Figures 8G–8I), but not at ROIs that were 30–60 µm away from ROI-1 (peak: 90.7% ± 5.8%; p = 0.020; area: 100.6% ± 8.1%; p = 0.925; n = 9; Figures 8G–8I). At intermediate distances (10–30 µm), peak calcium transients were not significantly affected, while the area under the curve was increased (peak: 110.9% ± 11.0%; p = 0.366; area: 137.3% ± 13.8%; p = 0.049; n = 9; Figure 8I). Thus, consistent with the triple-patch recordings, the imaging data show that dendritic plasticity may be restricted to the activated areas of the dendritic tree.

DISCUSSION

We have shown that synaptic or nonsynaptic stimulation protocols trigger plasticity of IE in the dendrites of cerebellar Purkinje cells. This amplification of dendritic signaling reflects downregulation of SK2 channel activity and can occur in a compartment-specific manner. Importantly, depolarizing current injections, nonsynaptic stimulations, enhance the amplitude of passively propagated Na^+ spikes, a nonsynaptic response. This demonstrates that the underlying mechanism is an alteration of intrinsic Purkinje cell properties.

The amplification of dendritic CF responses is likely to affect Purkinje cell output. CF signaling elicits widespread dendritic calcium transients, which, in PF-contacted spines, reach supralinear levels when PF and CF synapses are coactivated (Wang et al., 2000). Both LTD and LTP are calcium-triggered processes, but there is a higher calcium threshold for LTD than for LTP induction (Coesmans et al., 2004). CF coactivation therefore facilitates LTD induction, and additional alterations in CF and/or PF signaling will shift the induction probabilities for LTD and LTP. Our confocal imaging studies indeed show that CF-evoked calcium transients can be locally amplified in dendritic plasticity. Similarly, we have recently shown that repeated depolarizing current injections at 5 Hz for 3 s, one of the protocols that was also used in the present study, enhance PF-evoked spine calcium transients, and lower the probability for the subsequent induction of LTP (Belmeguenai et al., 2010). These data suggest that excitability changes in the dendrite result in altered calcium signaling and can modulate

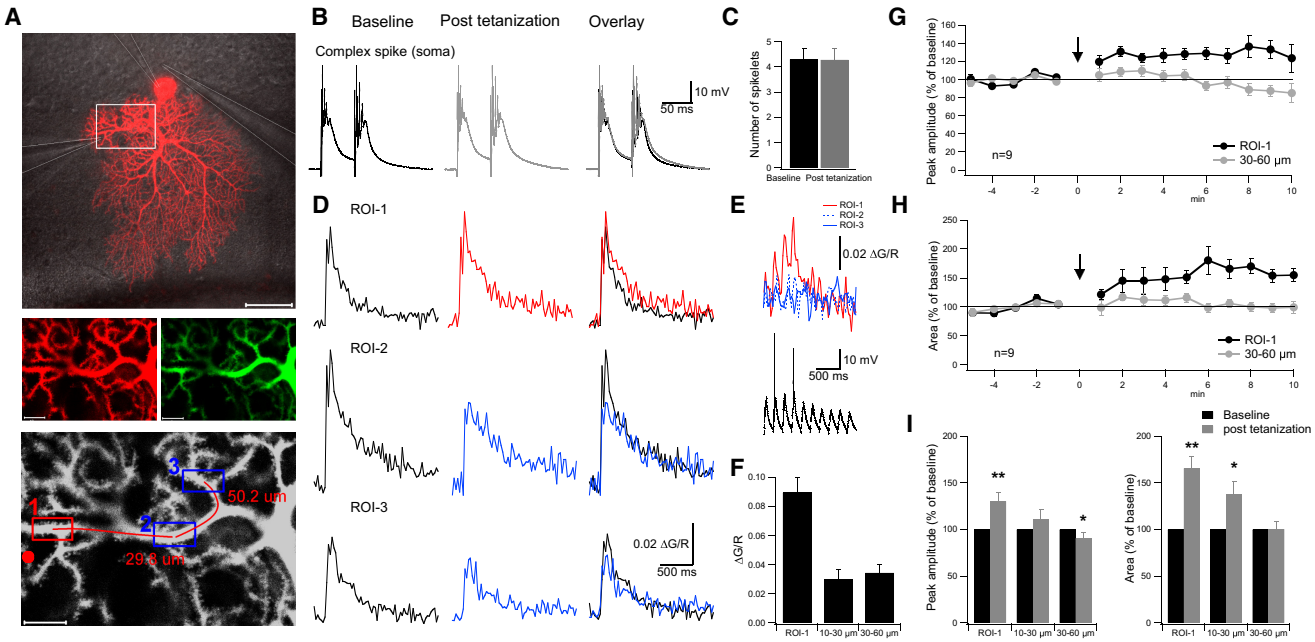

Figure 8. Confocal Calcium Imaging Shows Location-Specific Dendritic Plasticity

(A) Top: Purkinje cell filled with Alexa 633. The lines indicate the location of the somatic patch electrode as well as the glass pipettes that were used for PF (left) and CF stimulation (right). Scale bar: 50 µm. Middle: enlarged view of the area indicated by the white box in the top picture. Left: red fluorescence of Alexa 633 (30 µM). Right: green fluorescence of Oregon Green BAPTA-2 (200 µM). Scale bars: 10 µm. Bottom: image illustrating the location of the stimulus pipette (red dot), and of ROIs 1–3. The red line indicates the dendritic axis along which the distance of ROI-2 and -3 (center of the ROI box) from ROI-1 was determined. Scale bar: 10 µm.

(B) Complex spikes recorded during the baseline (left) and after tetanization (middle). Right: overlay of the traces.

(C) Weak PF activation did not change the number of spikelets in the complex spike waveform (n = 9).

(D) CF-evoked calcium transients at ROI-1 (top), ROI-2 (middle) and ROI-3 (bottom) before (left) and after tetanization (middle). Right: overlay of the traces.

(E) Top: calcium transients monitored during the PF tetanization protocol (first two seconds) at ROIs 1–3. Bottom: somatic response to PF tetanization. Stimulus artifacts and antidromic spikes were suppressed.

(F) Bar graphs indicate calcium transients evoked during PF tetanization at ROI-1 (≤10 µm distance from stimulus pipette), ROI-2 (10–30 µm distance from ROI-1), and ROI-3 (30–60 µm distance from ROI-1). Calcium transients were recorded during tetanization in 3/9 cells.

(G) Time graph showing changes in the peak amplitude of CF-evoked calcium transients after PF tetanization at ROI-1 and at ROIs located at a distance of 30–60 µm from ROI-1 (n = 9).

(H) Time graph showing corresponding changes in the area under the curve of CF-evoked calcium transients (n = 9).

(I) Left: bar graphs summarizing peak amplitude changes at ROI-1 as well as ROIs located at 10–30 µm and 30–60 µm distance from ROI-1, respectively (n = 9). Right: corresponding changes in the area under the curve (n = 9). Error bars indicate SEM. Asterisks indicate significant difference from baseline (paired Student's t test). *$p < 0.05$ and **$p < 0.01$.

the LTD/LTP balance. In addition, our previous study (Belmeguenai et al., 2010) showed that this form of intrinsic plasticity can be triggered by repeated current injections or PF tetanization, is measured as an increase in the number of depolarization-evoked spikes (see Figure 3) and is mediated, at least in part, by downregulation of SK channel activity (Belmeguenai et al., 2010; Hosy et al., 2011). Thus, it is possible that intrinsic plasticity in the soma and the dendrites share an underlying cellular mechanism. Intrinsic plasticity as recorded in Purkinje cell somata depends on postsynaptic calcium transients, the activation of protein phosphatases 1, 2A, and 2B, as well as the activation of protein kinase A (PKA) and protein kinase CK2 (Belmeguenai et al., 2010). PKA and CK2 have both been shown to directly downregulate SK2 channel activity, although by distinct molecular mechanisms. While PKA regulates the surface expression of SK2 channels (Lin et al., 2008), CK2 reduces their calcium sensitivity (Allen et al., 2007; Giessel and Sabatini, 2010).

In addition to its effect on dendritic processing, dendritic plasticity alters the complex spike waveform, increasing the number of spikelets. This, in turn, could increase the number of spikes that propagate down the axon. Previous studies have shown that the first and the last spikelets are most likely to successfully propagate, because of their relatively high amplitudes (Khaliq and Raman, 2005; Monsivais et al., 2005). The spikelets added as a result of enhanced dendritic IE are typically seen toward the end of the waveform (see Figure 2B) and might thus be reflected in the axonal spike pattern. Therefore, changes in the complex spike waveform will not only modify the Purkinje cell interpretation of CF activity, but might also change their electrical output function, affecting the inhibition of target neurons in the cerebellar nuclei (Aizenman and Linden, 1999; Pedroarena and Schwarz, 2003; Pugh and Raman, 2009).

PF responses are modified by dendritic plasticity, depending on the position of a PF-EPSP within an EPSP train. Due to paired-pulse facilitation, the amplitude of EPSPs increases

during an EPSP train. Our recordings show that dendritic plasticity does not enhance single PF-EPSPs. Rather, the enhanced excitability further amplifies EPSP facilitation within a train. This effect selectively boosts strong PF inputs and alters the filtering properties of the dendrite.

Modifications of intrinsic properties are based on changes in ion channel activity, and are known to alter dendritic response characteristics and signal processing (Fan et al., 2005; Frick et al., 2004; Lin et al., 2008; Nelson et al., 2005; Ramakers and Storm, 2002; Rancz and Häusser, 2010). Here we find that, similar to our previous study of somatically recorded IE plasticity (Belmeguenai et al., 2010), bath application of the highly selective SK channel blocker, apamin, mimics and occludes dendritic IE plasticity, as monitored by changes in CF responses, PF-EPSP trains and Na^+ spikes, suggesting a common underlying molecular process. Moreover, dendritic excitability changes were lost in *SK2*$^{-/-}$ mice, specifically implicating SK2-containing channels.

Apamin-sensitive SK channels activate rapidly with onset within 1 ms ($\tau \sim 10$ms in saturating calcium; Bond et al., 2004; Sah and Faber, 2002; Xia et al., 1998), sufficiently fast to affect the peak amplitude of CF responses (time to peak: 3.4 ms ± 0.1 SEM; n = 40; averaged baseline values from all rat recordings) as well as the amplitude of even the earliest Na^+ spikelets evoked by depolarizing current pulses. Thus, apamin bath application causes an increase in both parameters. It remains possible that SK channels may be located on CF terminals and additionally affect glutamate release. Nevertheless, both the plasticity of dendritic IE and apamin bath application were associated with an increase in the amplitude and frequency of depolarization-evoked Na^+ spikes, suggesting a postsynaptic modification. Moreover, release at CF synapses operates at near saturation (Dittman and Regehr, 1998), which makes a contribution by a presynaptic potentiation mechanism unlikely. Rather, the data suggest that a regulation of SK2 channels located on Purkinje cell dendrites mediates this form of intrinsic plasticity. It remains to be determined whether the increase in dendritic IE reflects changes in the biophysical properties of SK2 channels and/or reduced SK2 surface expression (Lin et al., 2008; Allen et al., 2007). Moreover, future work will have to address the question whether intermediate conductance calcium-activated K channels (Engbers et al., 2012) or large conductance BK-type K channels (Rancz and Häusser, 2006, 2010) play similar or complementary roles in activity-dependent plasticity of dendritic IE.

Triple-patch recordings were used to simultaneously monitor CF responses in the soma and at two dendritic locations. These experiments show that local activation by dendritic current injection or weak PF activation can trigger increases in dendritic IE that are restricted to the conditioned site. This observation was confirmed by our confocal imaging experiments, which show that local PF activation results in an amplification of CF-evoked calcium transients at the ROI closest to the stimulation site (ROI-1; $\leq$ 10 μm), but that this amplification is not seen at ROIs that are located 30–60 μm away from ROI-1. At intermediate distances (10-30 μm), CF responses were still enhanced on average, but to a lower degree than at ROI-1. In both types of experiments, local amplification of dendritic CF responses was used as a measure of excitability changes, because CF signaling provides large, widespread signals that can be recorded at multiple dendritic locations. In addition to its use as an indicator of dendritic plasticity, this location-specific amplification process is physiologically interesting, because an enhancement of the instructive CF signal and the associated calcium transient could locally affect the LTD/LTP balance at nearby PF synapses (Ohtsuki et al., 2009). It has previously been demonstrated in vivo that brief high-frequency bursts constitute a typical granule cell response to sensory stimulation (Chadderton et al., 2004). Thus, the PF burst pattern used (5 pulses at 50 Hz; repeated at 5 Hz for 3 s) likely provides a physiological input pattern, suggesting that the spatial restriction of dendritic plasticity reported here (on average no amplification at distances of > 30 μm from the conditioned site) reflects a physiologically relevant degree of localization. It should be noted, however, that this finding does not exclude the possibility that dendritic excitability changes can be even more spatially restricted.

In CA1 hippocampal pyramidal neurons, local changes in A-type K channels result in long-term adjustments of branch coupling strength that have been suggested to play a role in the storage of specific input patterns (Losonczy et al., 2008; Makara et al., 2009). Another study showed that A-type K channels and SK channels play complementary roles in limiting dendritic responses to the stimulated branch (Cai et al., 2004). However, there is a fundamental difference in the way that SK channels and voltage-gated K channels control dendritic responsiveness. SK channels are exclusively activated by calcium and, in turn, regulate the amplitude and kinetics of EPSPs and curtail spine calcium transients (Belmeguenai et al., 2010; Lin et al., 2008; Ngo-Anh et al., 2005). Thus, SK channel activation is part of a negative feedback loop that is closely tied to calcium signaling and provides a unique brake mechanism to influence dendritic processing. Our data provide the first demonstration that the gain of this dendritic brake mechanism may be adjusted in an activity-dependent way. Moreover, we show that this form of plasticity of dendritic IE can be restricted to selectively activated compartments of the dendrite. The concept of individual dendritic branches (or subcompartments of branches) as computational units of modification and memory storage is also highlighted in the Clustered Plasticity Hypothesis, which states that changes in synaptic strength preferentially occur at synapses that are clustered at discrete locations on the dendrite (Govindarajan et al., 2006, 2011). Activity-dependent clustered synaptic plasticity has been observed in neural circuit development as well as in young adult learning and might enable grouping of functionally related input patterns onto dendritic subcompartments (Fu et al., 2012; Kleindienst et al., 2011; Makino and Malinow, 2011; Takahashi et al., 2012). Together, these data show that forms of activity-dependent synaptic and nonsynaptic plasticity can selectively regulate dendritic input processing at the level of dendritic subdomains. In this scenario, SK2 channel plasticity might assume the role of a local amplification mechanism that participates in dendritic input gain control. The data presented here show that in Purkinje cell dendrites, SK2 channel plasticity provides such an additional, nonsynaptic gain control mechanism that could

complement LTD and LTP in information storage (Hansel et al., 2001; Jörntell and Hansel, 2006; Schonewille et al., 2011) and is an example of how active dendritic conductances contribute to the computational power of neurons.

EXPERIMENTAL PROCEDURES

Slice Preparation

Sagittal slices of the cerebellar vermis (220 μm) were prepared from Sprague-Dawley rats (P25–P37) after isoflurane anesthesia and decapitation. This procedure is in accordance with the guidelines of the Animal Care and Use Committees of the University of Chicago and Erasmus University. In some experiments, *SK2*$^{-/-}$ mice (Bond et al., 2004) and wild-type littermates (P17–P35) were used. Slices were cut on a vibratome (Leica VT1000S) using ceramic blades. Subsequently, slices were kept in ACSF containing the following (in mM): 124 NaCl, 5 KCl, 1.25 Na_2HPO_4, 2 $MgSO_4$, 2 $CaCl_2$, 26 $NaHCO_3$ and 10 D-glucose, bubbled with 95% O_2 and 5% CO_2.

Patch-Clamp Recordings

Slices recovered for at least 1 hr and were then transferred to a recording chamber superfused with ACSF at near-physiological temperature (31°C–34°C). The ACSF was supplemented with 100 μM picrotoxin to block $GABA_A$ receptors. Patch recordings were performed under visual control with differential interference contrast optics in combination with near-infrared light illumination (IR-DIC) using a Zeiss AxioCam MRm camera and a ×40 IR-Achroplan objective, mounted on a Zeiss Axioscope 2FS microscope (Carl Zeiss MicroImaging). Patch-clamp recordings were performed in current-clamp mode (Rs compensation off/fast capacitance compensation on) using an EPC-10 quadro amplifier (HEKA Electronics). Membrane voltage and current were filtered at 3 kHz, digitized at 25 kHz, and acquired using Patchmaster software (HEKA Electronics). Patch pipettes (borosilicate glass) were filled with a solution containing (in mM): 9 KCl, 10 KOH, 120 K-gluconate, 3.48 $MgCl_2$, 10 HEPES, 4 NaCl, 4 Na_2ATP, 0.4 Na_3GTP, and 17.5 sucrose (pH 7.25). Resting $[Ca^{2+}]_i$ determined under these experimental conditions was 67.3 ± 14.7 nM (n = 9; for technical details, see below). Membrane voltage was corrected for liquid junction potentials (11.7 mV). Somatic patch electrodes had electrode resistances of 2–5 MΩ, while dendritic patch electrodes had electrode resistances of 7–10 MΩ. Hyperpolarizing bias currents (100–350 pA) were injected to stabilize the membrane potential at about −75 mV and to prevent spike activity. Depolarizing current steps (250–400 pA/350–550 ms) were applied to the soma to evoke action potentials when experimentally required. For CF stimulation (4–12 μA/200 μs pulses), glass pipettes filled with ACSF were placed in the granule cell layer. For PF stimulation (1–8 μA/200 μs pulses), glass pipettes were placed in the molecular layer. To trigger widespread dendritic plasticity with the 50 Hz PF tetanization protocol (Figure 2D), the stimulus electrode was randomly placed in the molecular layer (dendritic response amplitude: 12.5 ± 1.0 mV; stimulus intensity: 13.4 ± 1.4 μA; n = 5). In contrast, to trigger local excitability changes (Figure 7), the stimulus electrode was placed lateral to one dendritic recording site (see Figure 7B), and the stimulus intensity was adjusted to evoke smaller PF-EPSPs (dendritic response amplitude: 5.3 ± 0.7mV; stimulus intensity: 19.5 ± 6.2 μA; n = 3; note different location of the stimulus electrode). Thus, the protocol attributes "weak" and "strong" were selected to refer to the dendritic response strength and do not reflect differences in the stimulus intensity/electrode location. In contrast to the imaging experiments, where stimulus pipettes could be placed very close to the dendritic target area (≤10 μm distance), stability of dendritic recordings required electrode placement at larger distances where the stimulus electrode would not interfere with the dendritic patch recordings (>20 μm distance). Spikelets (complex spike; dendritic Na^+ spikes) were identified as positive deflections in the somatic and dendritic recordings, respectively. The amplitude of dendritic Na^+ spikes was measured from the base of the action potentials as determined by a sudden acceleration of the depolarizing phase. Input resistance was monitored by injecting 100 pA and 20 pA hyperpolarizing pulses (50 ms duration) at the somatic and dendritic recording sites, respectively (Figure S3).

Confocal Calcium Imaging

Calcium transients were monitored using a Zeiss LSM 5 Exciter confocal microscope equipped with a ×63 Apochromat objective (Carl Zeiss MicroImaging). For calcium imaging experiments, sagittal slices of the cerebellar vermis (220 μm) were prepared from P20–P25 rats. Calcium transients were calculated as $\Delta G/R = (G(t) - G_0)/R$ (see Yasuda et al., 2004), where G is the calcium-sensitive fluorescence of Oregon Green BAPTA-2 (200 μM; G_0 = baseline signal), and R is the time-averaged calcium-insensitive fluorescence of Alexa 633 (30 μM). The green fluorescence G was excited at 488 nm using an argon laser (Lasos Lasertechnik). The red fluorescence R was excited during subsequent sweeps at 633 nm using a HeNe laser (Lasos Lasertechnik). Purkinje cells were loaded with Oregon Green BAPTA-2 and Alexa 633 by adding these dyes to the pipette solution. The experiments were initiated after the dendrite was adequately loaded with the dyes and the fluorescence at the selected ROIs reached a steady-state level, which typically required ≥ 30min. The recordings were performed at room temperature. Resting calcium levels were calculated as

$$[Ca2+] = K_D \frac{(G/R) - (G/R)\mathrm{min}}{(G/R)\mathrm{max} - (G/R)}$$

where K_D is the dissociation constant of Oregon Green BAPTA-2, and $(G/R)_{max}$ and $(G/R)_{min}$ are the fluorescence ratios at saturating and zero (external) calcium concentrations, respectively. For this calculation, we used the following values: K_D = 485 nM (cuvette measurements), G/R_{max} = 0.9440 (in situ measurement; injection of depolarizing currents in $[Ca^{2+}]_o$ = 4mM), and G/R_{min} = 0.0196 (in situ; no stimulation; $[Ca^{2+}]_o$ = 0 mM).

Data Analysis

Data were analyzed using Fitmaster software (HEKA Electronics) and Igor Pro software (WaveMetrics). Linearity was assessed by using Pearson's correlation coefficient, and statistical significance was determined by using the paired Student's t test (to test for significance of changes after an experimental manipulation in comparison to baseline) and the Mann-Whitney U test (between-group comparison), when appropriate. All data are shown as mean ± SEM.

SUPPLEMENTAL INFORMATION

Supplemental Information includes four figures and one table and can be found with this article online at http://dx.doi.org/10.1016/j.neuron.2012.05.025.

ACKNOWLEDGMENTS

This study was supported by grants from the National Institute of Neurological Disorders and Stroke (NS-062771 to C.H. and NS-038880 to J.P.A.), the Netherlands Organization for Scientific Research (NWO-ALW 817.02.013 to C.H.), and the Japanese Society for the Promotion of Science (JSPS 02714 to G.O.). We would like to thank S.M. Sherman, N. Spruston, and J. Waters for invaluable comments on the manuscript and laboratory members for helpful discussions.

Accepted: May 14, 2012
Published: July 11, 2012

REFERENCES

Aizenman, C.D., and Linden, D.J. (1999). Regulation of the rebound depolarization and spontaneous firing patterns of deep nuclear neurons in slices of rat cerebellum. J. Neurophysiol. *82*, 1697–1709.

Allen, D., Fakler, B., Maylie, J., and Adelman, J.P. (2007). Organization and regulation of small conductance Ca^{2+}-activated K^+ channel multiprotein complexes. J. Neurosci. *27*, 2369–2376.

Belmeguenai, A., Hosy, E., Bengtsson, F., Pedroarena, C.M., Piochon, C., Teuling, E., He, Q., Ohtsuki, G., De Jeu, M.T.G., Elgersma, Y., et al. (2010).

Intrinsic plasticity complements long-term potentiation in parallel fiber input gain control in cerebellar Purkinje cells. J. Neurosci. *30*, 13630–13643.

Bond, C.T., Herson, P.S., Strassmaier, T., Hammond, R., Stackman, R., Maylie, J., and Adelman, J.P. (2004). Small conductance Ca^{2+}-activated K^+ channel knock-out mice reveal the identity of calcium-dependent afterhyperpolarization currents. J. Neurosci. *24*, 5301–5306.

Cai, X., Liang, C.W., Muralidharan, S., Kao, J.P., Tang, C.M., and Thompson, S.M. (2004). Unique roles of SK and Kv4.2 potassium channels in dendritic integration. Neuron *44*, 351–364.

Chadderton, P., Margrie, T.W., and Häusser, M. (2004). Integration of quanta in cerebellar granule cells during sensory processing. Nature *428*, 856–860.

Cingolani, L.A., Gymnopoulos, M., Boccaccio, A., Stocker, M., and Pedarzani, P. (2002). Developmental regulation of small-conductance Ca^{2+}-activated K^+ channel expression and function in rat Purkinje neurons. J. Neurosci. *22*, 4456–4467.

Coesmans, M., Weber, J.T., De Zeeuw, C.I., and Hansel, C. (2004). Bidirectional parallel fiber plasticity in the cerebellum under climbing fiber control. Neuron *44*, 691–700.

Daoudal, G., and Debanne, D. (2003). Long-term plasticity of intrinsic excitability: learning rules and mechanisms. Learn. Mem. *10*, 456–465.

Davie, J.T., Kole, M.H., Letzkus, J.J., Rancz, E.A., Spruston, N., Stuart, G.J., and Häusser, M. (2006). Dendritic patch-clamp recording. Nat. Protoc. *1*, 1235–1247.

Davie, J.T., Clark, B.A., and Häusser, M. (2008). The origin of the complex spike in cerebellar Purkinje cells. J. Neurosci. *28*, 7599–7609.

Dittman, J.S., and Regehr, W.G. (1998). Calcium dependence and recovery kinetics of presynaptic depression at the climbing fiber to Purkinje cell synapse. J. Neurosci. *18*, 6147–6162.

Edgerton, J.R., and Reinhart, P.H. (2003). Distinct contributions of small and large conductance Ca^{2+}-activated K^+ channels to rat Purkinje neuron function. J. Physiol. *548*, 53–69.

Engbers, J.D.T., Anderson, D., Asmara, H., Rehak, R., Mehaffey, W.H., Hameed, S., McKay, B.E., Kruskic, M., Zamponi, G.W., and Turner, R.W. (2012). Intermediate conductance calcium-activated potassium channels modulate summation of parallel fiber input in cerebellar Purkinje cells. Proc. Natl. Acad. Sci. USA *109*, 2601–2606.

Faber, E.S.L., Delaney, A.J., and Sah, P. (2005). SK channels regulate excitatory synaptic transmission and plasticity in the lateral amygdala. Nat. Neurosci. *8*, 635–641.

Fan, Y., Fricker, D., Brager, D.H., Chen, X., Lu, H.C., Chitwood, R.A., and Johnston, D. (2005). Activity-dependent decrease of excitability in rat hippocampal neurons through increases in I(h). Nat. Neurosci. *8*, 1542–1551.

Frick, A., Magee, J., and Johnston, D. (2004). LTP is accompanied by an enhanced local excitability of pyramidal neuron dendrites. Nat. Neurosci. *7*, 126–135.

Fu, M., Yu, X., Lu, J., and Zuo, Y. (2012). Repetitive motor learning induces coordinated formation of clustered dendritic spines in vivo. Nature *483*, 92–95.

Giessel, A.J., and Sabatini, B.L. (2010). M1 muscarinic receptors boost synaptic potentials and calcium influx in dendritic spines by inhibiting postsynaptic SK channels. Neuron *68*, 936–947.

Govindarajan, A., Kelleher, R.J., and Tonegawa, S. (2006). A clustered plasticity model of long-term memory engrams. Nat. Rev. Neurosci. *7*, 575–583.

Govindarajan, A., Israely, I., Huang, S.Y., and Tonegawa, S. (2011). The dendritic branch is the preferred integrative unit for protein synthesis-dependent LTP. Neuron *69*, 132–146.

Hammond, R.S., Bond, C.T., Strassmaier, T., Ngo-Anh, T.J., Adelman, J.P., Maylie, J., and Stackman, R.W. (2006). Small-conductance Ca^{2+}-activated K^+ channel type 2 (SK2) modulates hippocampal learning, memory, and synaptic plasticity. J. Neurosci. *26*, 1844–1853.

Hansel, C., Linden, D.J., and D'Angelo, E. (2001). Beyond parallel fiber LTD: the diversity of synaptic and non-synaptic plasticity in the cerebellum. Nat. Neurosci. *4*, 467–475.

Häusser, M., Spruston, N., and Stuart, G.J. (2000). Diversity and dynamics of dendritic signaling. Science *290*, 739–744.

Hosy, E., Piochon, C., Teuling, E., Rinaldo, L., and Hansel, C. (2011). SK2 channel expression and function in cerebellar Purkinje cells. J. Physiol. *589*, 3433–3440.

Jörntell, H., and Hansel, C. (2006). Synaptic memories upside down: bidirectional plasticity at cerebellar parallel fiber-Purkinje cell synapses. Neuron *52*, 227–238.

Khaliq, Z.M., and Raman, I.M. (2005). Axonal propagation of simple and complex spikes in cerebellar Purkinje neurons. J. Neurosci. *25*, 454–463.

Kleindienst, T., Winnubst, J., Roth-Alpermann, C., Bonhoeffer, T., and Lohmann, C. (2011). Activity-dependent clustering of functional synaptic inputs on developing hippocampal dendrites. Neuron *72*, 1012–1024.

Lancaster, B., Hu, H., Ramakers, G.M.J., and Storm, J.F. (2001). Interaction between synaptic excitation and slow afterhyperpolarization current in rat hippocampal pyramidal cells. J. Physiol. *536*, 809–823.

Lin, M.T., Luján, R., Watanabe, M., Adelman, J.P., and Maylie, J. (2008). SK2 channel plasticity contributes to LTP at Schaffer collateral-CA1 synapses. Nat. Neurosci. *11*, 170–177.

Llinás, R., and Sugimori, M. (1980). Electrophysiological properties of in vitro Purkinje cell dendrites in mammalian cerebellar slices. J. Physiol. *305*, 197–213.

Losonczy, A., Makara, J.K., and Magee, J.C. (2008). Compartmentalized dendritic plasticity and input feature storage in neurons. Nature *452*, 436–441.

Magee, J.C., and Johnston, D. (2005). Plasticity of dendritic function. Curr. Opin. Neurobiol. *15*, 334–342.

Makara, J.K., Losonczy, A., Wen, Q., and Magee, J.C. (2009). Experience-dependent compartmentalized dendritic plasticity in rat hippocampal CA1 pyramidal neurons. Nat. Neurosci. *12*, 1485–1487.

Makino, H., and Malinow, R. (2011). Compartmentalized versus global synaptic plasticity on dendrites controlled by experience. Neuron *72*, 1001–1011.

Monsivais, P., Clark, B.A., Roth, A., and Häusser, M. (2005). Determinants of action potential propagation in cerebellar Purkinje cell axons. J. Neurosci. *25*, 464–472.

Nelson, A.B., Gittis, A.H., and du Lac, S. (2005). Decreases in CaMKII activity trigger persistent potentiation of intrinsic excitability in spontaneously firing vestibular nucleus neurons. Neuron *46*, 623–631.

Ngo-Anh, T.J., Bloodgood, B.L., Lin, M., Sabatini, B.L., Maylie, J., and Adelman, J.P. (2005). SK channels and NMDA receptors form a Ca^{2+}-mediated feedback loop in dendritic spines. Nat. Neurosci. *8*, 642–649.

Ohtsuki, G., Piochon, C., and Hansel, C. (2009). Climbing fiber signaling and cerebellar gain control. Front. Cell. Neurosci. *3*, 4.

Pedroarena, C.M., and Schwarz, C. (2003). Efficacy and short-term plasticity at GABAergic synapses between Purkinje and cerebellar nuclei neurons. J. Neurophysiol. *89*, 704–715.

Pugh, J.R., and Raman, I.M. (2009). Nothing can be coincidence: synaptic inhibition and plasticity in the cerebellar nuclei. Trends Neurosci. *32*, 170–177.

Ramakers, G.M.J., and Storm, J.F. (2002). A postsynaptic transient K(+) current modulated by arachidonic acid regulates synaptic integration and threshold for LTP induction in hippocampal pyramidal cells. Proc. Natl. Acad. Sci. USA *99*, 10144–10149.

Rancz, E.A., and Häusser, M. (2006). Dendritic calcium spikes are tunable triggers of cannabinoid release and short-term synaptic plasticity in cerebellar Purkinje neurons. J. Neurosci. *26*, 5428–5437.

Rancz, E.A., and Häusser, M. (2010). Dendritic spikes mediate negative synaptic gain control in cerebellar Purkinje cells. Proc. Natl. Acad. Sci. USA *107*, 22284–22289.

Sah, P. (1996). Ca(2+)-activated K^+ currents in neurones: types, physiological roles and modulation. Trends Neurosci. *19*, 150–154.

Sah, P., and Faber, E.S.L. (2002). Channels underlying neuronal calcium-activated potassium currents. Prog. Neurobiol. *66*, 345–353.

Schonewille, M., Gao, Z., Boele, H.J., Veloz, M.F., Amerika, W.E., Simek, A.A.M., De Jeu, M.T., Steinberg, J.P., Takamiya, K., Hoebeek, F.E., et al. (2011). Reevaluating the role of LTD in cerebellar motor learning. Neuron *70*, 43–50.

Sourdet, V., Russier, M., Daoudal, G., Ankri, N., and Debanne, D. (2003). Long-term enhancement of neuronal excitability and temporal fidelity mediated by metabotropic glutamate receptor subtype 5. J. Neurosci. *23*, 10238–10248.

Stackman, R.W., Hammond, R.S., Linardatos, E., Gerlach, A., Maylie, J., Adelman, J.P., and Tzounopoulos, T. (2002). Small conductance Ca^{2+}-activated K^+ channels modulate synaptic plasticity and memory encoding. J. Neurosci. *22*, 10163–10171.

Stocker, M., Krause, M., and Pedarzani, P. (1999). An apamin-sensitive Ca^{2+}-activated K^+ current in hippocampal pyramidal neurons. Proc. Natl. Acad. Sci. USA *96*, 4662–4667.

Stuart, G., and Häusser, M. (1994). Initiation and spread of sodium action potentials in cerebellar Purkinje cells. Neuron *13*, 703–712.

Takahashi, N., Kitamura, K., Matsuo, N., Mayford, M., Kano, M., Matsuki, N., and Ikegaya, Y. (2012). Locally synchronized synaptic inputs. Science *335*, 353–356.

Wang, S.S.H., Denk, W., and Häusser, M. (2000). Coincidence detection in single dendritic spines mediated by calcium release. Nat. Neurosci. *3*, 1266–1273.

Womack, M.D., and Khodakhah, K. (2003). Somatic and dendritic small-conductance calcium-activated potassium channels regulate the output of cerebellar Purkinje neurons. J. Neurosci. *23*, 2600–2607.

Xia, X.M., Fakler, B., Rivard, A., Wayman, G., Johnson-Pais, T., Keen, J.E., Ishii, T., Hirschberg, B., Bond, C.T., Lutsenko, S., et al. (1998). Mechanism of calcium gating in small-conductance calcium-activated potassium channels. Nature *395*, 503–507.

Yasuda, R., Nimchinsky, E.A., Scheuss, V., Pologruto, T.A., Oertner, T.G., Sabatini, B.L., and Svoboda, K. (2004). Imaging calcium concentration dynamics in small neuronal compartments. Sci. STKE *2004*, pl5.

Zhang, W., and Linden, D.J. (2003). The other side of the engram: experience-driven changes in neuronal intrinsic excitability. Nat. Rev. Neurosci. *4*, 885–900.